

Comparative Thermal Inactivation Analysis of *Aspergillus oryzae* and *Thiellavia terrestris* Cutinase: Role of Glycosylation

Abhijit N. Shirke,^{1,2} An Su,^{1,2} J. Andrew Jones,^{2,3} Glenn L. Butterfoss,⁴ Mattheos A.G. Koffas,^{2,3} Jin Ryouon Kim,⁵ Richard A. Gross^{1,2}

¹Department of Chemistry and Chemical Biology, Rensselaer Polytechnic Institute, Troy, New York; telephone: +518-276-3734; fax: +518-276-3405; e-mail: grossr@rpi.edu

²Center for Biotechnology and Interdisciplinary Studies, Rensselaer Polytechnic Institute, Troy, New York

³Department of Chemical and Biological Engineering, Rensselaer Polytechnic Institute, Troy, New York

⁴Center for Genomics and Systems Biology, New York University Abu Dhabi, Abu Dhabi, UAE

⁵Department of Chemical and Biomolecular Engineering, New York University Tandon School of Engineering, Brooklyn, New York; telephone: +646-997-3719; fax: +646-997-3136; e-mail: jin.kim@nyu.edu

ABSTRACT: Cutinase thermostability is important so that the enzymes can function above the glass transition of what are often rigid polymer substrates. A detailed thermal inactivation analysis was performed for two well-characterized cutinases, *Aspergillus oryzae* Cutinase (AoC) and *Thiellavia terrestris* Cutinase (TtC). Both AoC and TtC are prone to thermal aggregation upon unfolding at high temperature, which was found to be a major reason for irreversible loss of enzyme activity. Our study demonstrates that glycosylation stabilizes TtC expressed in *Pichia pastoris* by inhibiting its thermal aggregation. Based on the comparative thermal inactivation analyses of non-glycosylated AoC, glycosylated (TtC-G), and non-glycosylated TtC (TtC-NG), a unified model for thermal inactivation is proposed that accounts for thermal aggregation and may be applicable to other cutinase homologues. Inspired by glycosylated TtC, we successfully employed glycosylation site engineering to inhibit AoC thermal aggregation. Indeed, the inhibition of thermal aggregation by AoC glycosylation was greater than that achieved by conventional use of trehalose under a typical condition. Collectively, this study demonstrates the excellent potential of implementing glycosylation site engineering for thermal aggregation inhibition, which is one of the most common reasons for the irreversible thermal inactivation of cutinases and many proteins. *Biotechnol. Bioeng.* 2016;9999: 1–11.

© 2016 Wiley Periodicals, Inc.

KEYWORDS: thermal inactivation; aggregation; glycosylation; cutinase

Introduction

The industrial application of enzymes is often limited due to low stability under relevant reaction conditions. In this context, stability is defined by resistance to denaturation or loss of activity caused by stresses such as temperature, pressure, and exposure to chemical denaturants. These stressors may lead to protein unfolding, degradation, chemical modification, and aggregation resulting in the loss of enzyme activity (Bennion and Daggett, 2003; Carrion-Vazquez et al., 1999; Chi et al., 2003; Fagain, 1995; Fields, 2001; Hayakawa et al., 1996; Shortle, 1996). Protein stability in aqueous solutions is governed by complex interactions among amino acid side chains, backbones, as well as solvent molecules (Matthews, 1993; Pace, 1992; Robertson and Murphy, 1997; Timasheff, 1993). Many of these interactions are highly sensitive to environmental conditions such as pH, temperature, and ionic strength (Otzen, 2002; Somero, 1995; Yang and Honig, 1993). Enzyme thermostability is frequently desirable, as more productive reaction kinetics are generally favored at high temperatures (Leskovic, 2003; Sizer, 2006). Thermostability is often defined by an enzyme's thermal unfolding temperature, however, in the context of industrial applications, the kinetic stability, as given by the half-life of the active enzyme under suitable reaction conditions, is also very important (Polizzi et al., 2007; Sanchez-Ruiz, 2010).

Protein engineering has proven effective at improving protein stability, where stabilization is mainly achieved by: (i) decreasing the relative entropic difference between the folded protein and the unfolded ensemble (entropic stabilization); (ii) lowering the relative energy of the folded state (enthalpic stabilization); and (iii) inhibition of aggregation (Mozhaev, 1993; Yang et al., 2015). A number of wild type thermophilic proteins exploit these stabilization strategies by virtue of several structural features such as the presence of prolines in loop regions, disulfide bonds,

Abhijit N. Shirke and An Su have contributed equally to this work.

Correspondence to: R. A. Gross and J. R. Kim

Received 3 April 2016; Revision received 1 July 2016; Accepted 11 July 2016

Accepted manuscript online xx Month 2016;

Article first published online in Wiley Online Library (wileyonlinelibrary.com).

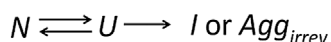
DOI 10.1002/bit.26052

and surface salt bridges (Fields, 2001; Querol et al., 1996; Vieille and Zeikus, 2001). Glycosylation is another feature of eukaryotic proteins that frequently contributes to stability (Fonseca-Maldonado et al., 2013; Shental-Bechor and Levy, 2008; Wang et al., 1996). The mechanism of stabilization by glycosylation could be either entropic (DeKoster and Robertson, 1997; Imperiali and O'Connor, 1999), enthalpic (Shental-Bechor and Levy, 2008), inhibition of aggregation (Høiberg-Nielsen et al., 2006, 2009), or by a combination of these mechanisms.

Apart from these protein engineering strategies, chemical additives have proven to be useful for thermostabilization. Several additives, primarily polyols and sugars, have shown to produce significant improvements in the kinetic stability of enzymes at both storage and reaction conditions (Arakawa and Timasheff, 1982, 1985; Kaushik and Bhat, 1998). These additives primarily function by the excluded volume effect, lowering water activity, and thereby inhibiting enzyme aggregation (Arakawa and Timasheff, 1985; Baynes and Trout, 2004; Devi and Rao, 1998; Gouda et al., 2003; Jain and Roy, 2009).

Cutinases are esterases of significant industrial importance due to their ability to hydrolyze a wide range of synthetic polyesters such as polycaprolactone (PCL), polyethylene terephthalate (PET), polybutylene succinate (PBS) (Baker et al., 2012; Chen et al., 2013; Pio and Macedo, 2009). These biotransformations can be used for polyester surface modifications (Eberl et al., 2009; Gübitz and Paulo, 2003; Lee and Song, 2010; Vertommen et al., 2005; Zhang et al., 2012) and may provide mild routes for the recycling of commodity polyesters to their corresponding monomers (Barth et al., 2015; Wei et al., 2013). Cutinases have also shown utility in small molecule ester synthesis (De Barros et al., 2009, 2012) and transesterification reactions (Badenes et al., 2010; Carvalho et al., 2000; Kazenwadel et al., 2012).

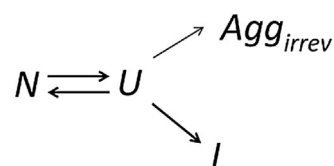
An in-depth understanding of the inactivation mechanism provides guidelines for protein engineering strategies to improve stability (Mozhaev, 1993). Thermal inactivation of a number of proteins, including *Fusarium solani* cutinase (FsC) at pH 9, is described by the Lumry–Eyring mechanism (Lumry and Eyring, 1954; Sanchez-Ruiz, 1992) (Scheme 1) where: *N* is the native state, *U* is the reversibly unfolded state, *I* is the irreversibly unfolded state, and *Agg_{irrev}* is the irreversibly aggregated state.



Scheme 1.

The first step is reversible unfolding followed by an irreversible inactivation. The irreversible inactivation step is mainly caused by either irreversible unfolding, aggregation, or chemical modifications at higher temperatures (Lumry and Eyring, 1954). Amongst cutinases, the thermal inactivation mechanism of FsC was studied in detail by Baptista et al. (2003). At pH 4.5, the enzyme was reported to undergo thermal unfolding to the reversibly unfolded state *U* followed by two parallel irreversible steps: thermal aggregation (*Agg_{irrev}*) or irreversible unfolding (*I*) (Scheme 2).

The cutinase from *Aspergillus oryzae* (AoC) is a promising enzyme for polyester hydrolysis, owing to an extended groove near



Scheme 2.

its active site which allows polymer substrates better catalytic access (Liu et al., 2009). Also, the cutinase from *Thiellavia terrestris* (TtC) is notable for its ability to retain stability and activity in acidic media, which is desirable as the pH of the reaction medium during polyester hydrolysis tends to decrease with the continual generation of acidic reaction products (Yang et al., 2013). We previously explained that the differences in pH stability of AoC and TtC is based on contributions of surface charge interactions to the free energy of unfolding (Shirke et al., 2016). Apart from differences in the pH stability, AoC and TtC differ in terms of the presence of glycosylation. TtC has two putative N-linked glycosylation sites (Asn-Xxx-Ser/Thr where Xxx could be any amino acid but Pro) which is the common post translational modification for eukaryotes; AoC do not have any N-linked glycosylation sites.

This paper provides a detailed analysis of AoC and TtC thermal inactivation in a comparative manner. The relatively high sequence identity (56%) of AoC and TtC along with differences in their pH stability and presence of glycosylation provides an opportunity to gain insights into the protein sequence/structure features contributing to inactivation pathways. The analyses were performed at the respective optimum pH values. Thermal aggregation was found to play a major role in the inactivation of AoC and nonglycosylated TtC (TtC-NG). The glycosylated TtC (TtC-G) on the other hand was found to be very stable against thermal aggregation. Taking a lesson from TtC-G, the glycosylation site engineering was investigated as a strategy for stabilization of AoC against thermal aggregation in comparison to stabilization by trehalose.

Materials and Methods

Materials and Methods are placed in the supplementary information.

Results and Discussions

Thermal Inactivation of *Aspergillus oryzae* Cutinase (AoC)

Thermal inactivation of AoC was analyzed by residual activity for functional changes, DLS for aggregate formation and CD for conformational changes. The apparent T_m , determined by the midpoint of the thermal transition measured by a CD thermal scan, was used to analyze thermal inactivation. Analysis at T_m provides information about both the reversibility of inactivation upon cooling and the fate of the unfolded state after extended incubation (e.g., aggregation or irreversible unfolding). For this analysis with AoC, pH 8 was chosen as it is the optimum pH for both activity and stability

(Baker et al., 2012). At pH 8, the T_m for AoC from a CD temperature scan is 61°C (Fig. S1). The LCMS analysis of intact AoC both before and after thermal inactivation analysis excluded any possible role of chemical modifications such as deamidation and oxidation reactions contributing to thermal inactivation (data not shown).

Residual activity analysis provides information on the kinetics of thermal inactivation. Upon incubation at 61°C (apparent T_m), AoC undergoes thermal inactivation in a concentration dependent manner (Fig. 1A). Interestingly, at higher protein concentrations (50, 75, and 90 μM), the loss of residual activity follows a two-step thermal inactivation where a rapid decay occurs during the initial incubation period (1–1.5 h) followed by a slow inactivation upon further incubation (Figs. 1A and S2). A similar two step thermal deactivation has been reported for FsC which occurs even at 10 μM enzyme concentration (Baptista et al., 2003). The authors attributed this two-step behavior to the possible role of aggregation in addition to the irreversible thermal unfolding. In particular, they proposed that the initial rapid inactivation is caused by the concentration-dependent thermal aggregation (Baptista et al., 2003). To further investigate the role of thermal aggregation in AoC inactivation, a DLS analysis was performed.

Indeed, DLS analysis revealed that incubation at 61°C (apparent T_m) results in aggregation. AoC at all concentrations tested was found to first undergo rapid association to form agglomerates of varying size, depending on protein concentration (Fig. 1B). These aggregates were found to be soluble and also dissociable upon cooling, as determined by the reduction in intensity of scattered light, and are designated as Agg_{rev} (Table SI). However, reduction in the intensity of scattered light does not conclusively show that total recovery to the monomeric state occurs as it is difficult for DLS to distinguish protein in monomeric form from other small multi-meric states. Although, the differences in the scattered light intensity after cooling from Agg_{rev} for different concentrations indicates incomplete recovery of the monomeric species (Table SI). For more conclusive data, size exclusion chromatography (SEC) analysis was performed. Indeed, compared to the control samples, SEC analysis after incubation at the T_m and subsequent cooling revealed the presence of some high molecular weight aggregates (Fig. S3). Albeit, this analysis cannot be used to quantitatively describe the possible dissociation of aggregates due to dilution during the SEC analysis. Upon further incubation of the protein after rapid association at T_m (see above), the formation of large insoluble aggregates is revealed by sudden increases in size by DLS (Fig. 1B). In fact, at higher concentrations ($\geq 50 \mu\text{M}$), the formation of larger aggregates is evident by visual inspection. These aggregates remained insoluble even after cooling, and, therefore, are referred to as irreversible aggregates (Agg_{irrev}). The formation of irreversible aggregates is likely initiated by certain threshold concentration and size of Agg_{rev} . Indeed, irreversible aggregate formation occurred at different times depending on the protein concentration (e.g., ~ 0.75 h for 90 μM , ~ 1.75 h for 50 μM , and ~ 3.0 h for 10 μM) (Fig. 1B).

Protein aggregation usually occurs after unfolding, when the more hydrophobic surface area is exposed (Yan et al., 2003). At temperatures significantly lower than that necessary for the onset of unfolding (i.e., $< 40^\circ\text{C}$), AoC did not show any aggregation for more than 24 h (data not shown). In contrast, at temperatures above the

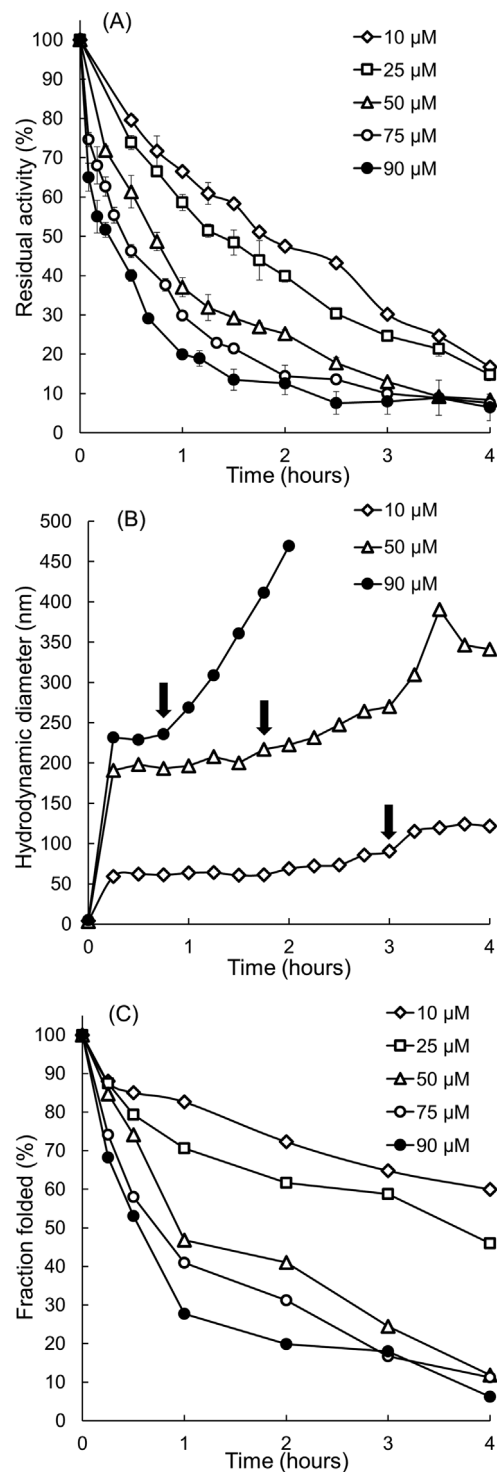


Figure 1. Thermostability analysis of wt-AoC at 61°C (apparent T_m) as a function of protein concentration: (A) residual activity analysis; (B) thermal aggregation analysis using DLS where the arrows indicate the onset of irreversible aggregation; and (C) residual secondary structure analysis by CD. Continuous lines are used to guide the eyes.

T_m , the content of unfolded species exceeds 50% and, correspondingly, the rate of the aggregation is very high which, in turn, leads to rapid loss of enzyme activity (Fig. S4 A and B). Thus, in the case of AoC, thermal unfolding was found to contribute to protein

aggregation which then leads to irreversible inactivation upon formation of irreversible aggregates.

However, the argument that irreversible inactivation occurs solely based on thermal aggregation is not supported by the loss of enzyme activity under conditions at which no irreversible aggregates have been formed (Fig. 1A and B). This indicates the possibility that alternative inactivation pathway occurs concurrently with thermal aggregation. Indeed, Baptista et al. (2003) reported a parallel inactivation profile for FsC at pH 4.5 where the protein undergoes irreversible inactivation by irreversible thermal unfolding concurrently with irreversible thermal aggregation. To probe the irreversible loss of the AoC structure as function of time at 61°C (apparent T_m), analysis of the secondary structure was performed by CD (Fig. 1C). The analysis revealed a consistent loss of secondary structure with incubation time, which follows a similar trend to that of residual activity (Fig. 1A and C). During the late stages of incubations, the observed loss of CD signals may be attributed not only to thermal unfolding but also a decrease in soluble protein concentration resulting from irreversible aggregation (Benjwal et al., 2006). Thus, in order to accurately evaluate the protein concentration dependency of irreversible thermal unfolding, we only considered inactivation data before formation of irreversible aggregates.

Unlike previous studies on FsC (Baptista et al., 2003), the loss of AoC secondary structure is concentration dependent. The concentration dependence of thermal unfolding also explains the concentration dependence of residual activity prior to formation of Agg_{irrev} (Fig. 1A). The concentration dependent loss of enzyme activity before the formation of irreversible aggregates can also be explained by the concentration effect on the reversibility of Agg_{rev} . As discussed earlier, Agg_{rev} did not completely dissociate to the monomeric state and larger extents of dissociation occurred at lower protein concentrations (Table SI). Thus, it is likely that the reversibility is further lowered with relatively large Agg_{rev} formed at higher concentrations resulting in the lower activity recovery upon cooling.

In summary, Scheme 3 below was formulated to capture the above aspects of AoC's thermal inactivation pathways:



Scheme 3.

where, N is the native state, U is the reversibly unfolded state, Agg_{rev} is reversible aggregates, Agg_{irrev} is irreversible aggregates, and I is the irreversibly unfolded state. Upon incubation at T_m , a fraction of protein molecules undergoes irreversible thermal unfolding while, in parallel, the rest follows the aggregation pathway. While thermal unfolding can be concentration-dependent, thermal aggregation is likely to follow a higher order process given the consideration of the size of aggregates shown in Figure 1B.

Thermal Inactivation of *Thiellavia terrestris* Cutinase

Thiellavia terrestris cutinase (TtC) is a fungal enzyme and, owing to the presence of two glycosylation sites (N195 and N123), it naturally exists in a glycosylated form (TtC-G) (Shirke et al., 2016). To evaluate the role of glycosylation on TtC-G thermostability, comparative thermal inactivation analyses of TtC-G and TtC-NG were performed. TtC-G and TtC-NG were successfully expressed in *Pichia pastoris* and *Escherichia coli*, respectively. As we previously reported, analysis of CD and intrinsic tryptophan fluorescence spectra led us to conclude that TtC-G and TtC-NG display similar secondary and tertiary structures (Shirke et al., 2016).

Thermal inactivation analysis of TtC-G and TtC-NG was performed similarly to AoC from residual activity, DLS and CD studies. For TtC, these experiments were performed at pH 5 since it is the optimum pH for TtC activity and stability (Yang et al., 2013). Figure 2 displays CD temperature scans to determine the T_m . Interestingly, TtC-G thermal unfolding occurs in two distinct steps. In the first step that occurs from 25 to 58°C, the native protein slowly unfolds to an intermediate state. Thereafter, from 58 to 70°C, the second step occurs where TtC-G undergoes a transition to the final unfolded state. The midpoint of the second transition at $67 \pm 0.5^\circ\text{C}$ was taken as the apparent T_m . The similar two step thermal transition has been reported in case of ribonuclease s where the first step was considered as the pre-transitional change (Stelea and Keiderling, 2002). In contrast to TtC-G the CD thermal scan of TtC-NG has a single sharp transition and the corresponding apparent T_m is $64 \pm 0.25^\circ\text{C}$. The glycosylation contributes to slight but significant (2–3°C) increase in the temperature of thermal unfolding which is consistent with the literature which suggests improvements in T_m caused by glycosylation are generally in the range of 1–6°C (Høiberg-Nielsen et al., 2006; Shental-Bechor and Levy, 2008; Solá et al., 2006; Tams and Welinder, 1998, 2001).

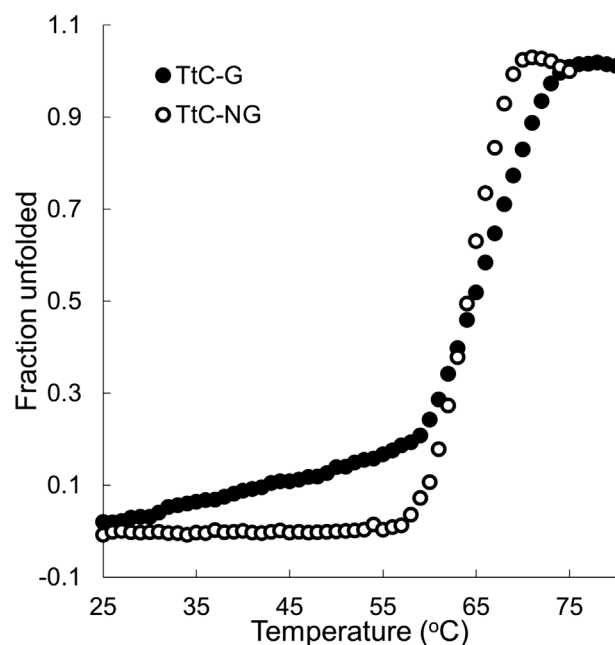
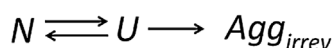


Figure 2. CD temperature scans to analyze TtC-G and TtC-NG thermal unfolding.

The residual activity analysis of TtC-NG revealed that incubation at 64°C (apparent T_m) results in rapid loss in enzyme activity with half-life times of 0.25, 0.18, and 0.16 h for protein concentrations of 10, 25, and 50 μM , respectively (Fig. 3A, Table SII). This rapid loss of activity was found to result from prompt irreversible aggregation that brings about precipitation. Indeed, the formation of precipitate was evident from visual observations at all assessed protein concentrations. It was difficult to obtain information on aggregate size since extensive aggregation causes low soluble protein concentrations. Hence, in order to obtain aggregation kinetic data, the intensity of scattered light was used (Fig. 3B). These higher rates of thermal induced aggregation are consistent with the rapid loss of enzyme activity (Fig. 3A and B). These results implicate that, for TtC, thermal aggregation is the primary deactivation mechanism. We believe that unfolding of TtC-NG is the primary cause of thermal aggregation as aggregation becomes prevalent at the onset of thermal unfolding at 60°C (Figs. S5 and S6). Where aggregation occurs at higher rates with increasing temperature (Fig. S5), it is negligible at temperatures below the onset of thermal unfolding. This is evident from scattered light intensity that remained unchanged at 40°C for incubations beyond 24 h (data not shown). Rapid irreversible aggregation and corresponding light scattering prevented the evaluation by CD of secondary structure loss kinetics.

The thermal inactivation of TtC-NG follows the pathway described in Scheme 4 where the native protein (N) first undergoes thermal unfolding (U) followed by formation of irreversible aggregates (Agg_{irrev}). As observed for AoC (Scheme 3), I or Agg_{rev} forms of TtC-NG may exist, however, the rapid formation by TtC-NG of Agg_{irrev} makes it difficult to track these species. LC-MS analysis shows that TtC chains remain intact during the incubations under the conditions used for the above analysis excluding the



Scheme 4.

potential role of chemical degradation reactions in thermal inactivation (data not shown).

Further, the potential effects of glycosylation on TtC thermostabilization were studied (Fig. 4A–C). Surprisingly, the DLS temperature scan of TtC-G showed no transitions in the intensity of the scattered light even up to 85°C (max temperature tested) where a clear transition to form aggregated species is observed for TtC-NG that begins at the onset of unfolding (Fig. S6). Furthermore, the DLS analysis of TtC-G at varying concentrations and temperatures revealed a high resistance to thermal aggregation. The protein retains its monomeric state throughout its thermal deactivation at 67°C (Fig. 4B). Indeed, the experimental hydrodynamic radius determined by DLS at 25°C and 25 μM is 4.2 ± 0.7 nm whereas the theoretical hydrodynamic radius of monomeric TtC-NG is 2–3 nm. Previous work has shown that the slightly larger hydrodynamic radius for TtC-G relative to TtC-NG may be due to glycosylation (Zhong and Somers, 2012). Furthermore, the SEC analysis of TtC-G samples incubated 4 h at 50 μM protein concentration and the apparent T_m confirmed that high molecular weight species did not form (Fig. S7).

Previous studies reported that protein glycosylation can increase protein solubility and inhibit thermal aggregation (Solá and Griebenow, 2010). However, it is exceptional for glycosylation to cause complete inhibition of thermal aggregation throughout TtC thermal deactivation. This may be due to glycosylation occurring at the optimal locations and extent. Multiple studies are available demonstrating the significance of both protein sequence and location of glycosylation site on the stabilization by glycosylation (Ellis et al., 2012; Fonseca-Maldonado et al., 2013). In particular, a systematic study conducted by Solá et al. (2006) demonstrated that glycosylation results in inhibition of protein–protein interactions by steric constrains. We believe that the high resistance of TtC-G to thermal aggregation is due to a similar stabilizing effect at an effective location in the protein sequence.

Consistent with stabilization against thermal aggregation, the residual activity analyses of TtC-G, performed at 67°C (apparent T_m), revealed a significantly higher kinetic stability relative to TtC-NG (Figs. 3A and 4A). The half-life time for thermal inactivation of TtC-G is ~ 13 –15 times longer than TtC-NG at

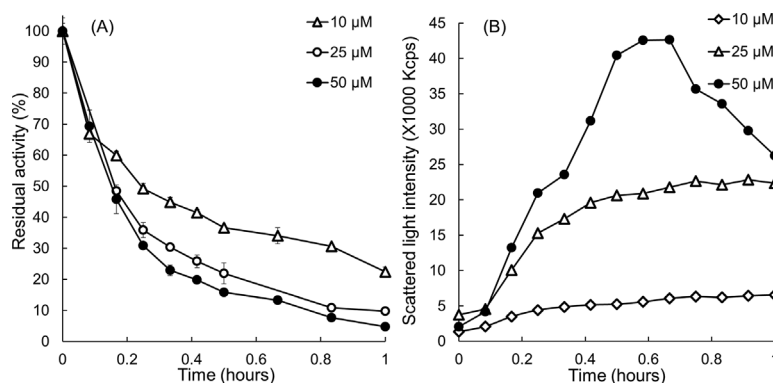


Figure 3. Analysis for TtC-NG at 64°C with varying concentration of (A) residual activity analysis; and (B) aggregation kinetics. Continuous lines are used to guide the eyes.

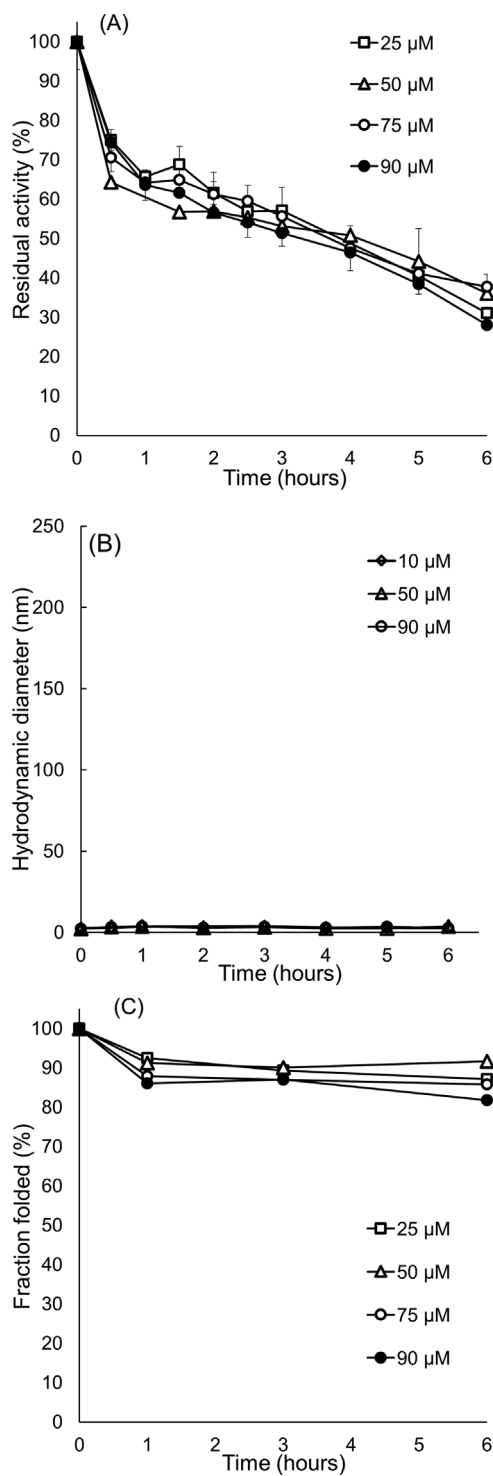


Figure 4. Thermal inactivation analysis of TtC-G at 67°C (apparent T_m): (A) residual activity; (B) aggregation kinetics using DLS; and (C) residual secondary structure using CD. Continuous lines are used to guide the eyes.

25–50 μM when measured at their respective T_m s (67 and 64°C) (Table SII). The apparent T_m s were chosen for the incubation to be consistent with the equal amount of the native state (50% at the T_m). It should be noted that higher incubation temperature

used for TtC-G should be kinetically more destabilizing, further supporting substantial stabilizing effects of glycosylation. The absence of aggregation for TtC-G also results in a similar rate of thermal inactivation at different concentrations (Fig. 4). Similar improvements in kinetic stability have been reported by glycosylation of proteins from other families (e.g., phytase (Høiberg-Nielsen et al., 2006), chymotrypsin (Solá et al., 2006), peroxidases (Tams and Welinder, 1998, 2001), etc).

In the absence of aggregation, irreversible thermal inactivation of TtC-G is likely due to irreversible alteration of the monomeric state's conformation. Indeed, the loss of secondary structure determined by CD, upon incubation at T_m , showed the loss of secondary structure (Fig. 4C). The secondary structure change is not as significant as the loss of activity. However, small structural changes can attribute to large losses in activity. Furthermore, CD analysis is limiting in terms of detecting minute structural changes that can lead to activity loss (Fig. 4A and C). Similar thermal denaturation to the inactive unfolded state with the residual structure has been reported in case of glycosylated glucose oxidase (Zoldák et al., 2004). The thermal inactivation of TtC-G, as determined by residual activity analysis, undergoes a two-step process where the initial drop in activity to 60–70% occurs rapidly (<1 h) and, thereafter, as the incubation time is extended, thermal deactivation occurs at a slower rate reaching 30–40% residual activity at 6 h. This residual activity profile is independent of the TtC-G concentrations tested (10, 50, and 90 μM) (Fig. 4A). The observed two-step TtC-G deactivation may be due to “kinetic entrapment” that can occur by rapid cooling. To test for this, 100 μL aliquots of protein solutions were withdrawn from incubations and immediately quenched in ice. In the case of shallow kinetic entrapment, the native state can be recovered upon prolonged incubation on ice after rapid cooling (Koutsopoulos et al., 2007; Rodriguez-Larrea et al., 2007). However, for TtC-G, prolonged incubation on ice did not lead to further recovery of enzyme activity, indicating that deep kinetic entrapment occurred. In other words, under these experimental conditions, TtC-G cannot fold back to the native state leaving a majority of the protein in a kinetically trapped state (referred to as the *P* state). The presence of glycans could force this trapping since this phenomenon was not observed for non-glycosylated TtC. This state (*P*) may be similar to the partially unfolded form of TtC-G that was observed in the CD thermal scan (Fig. 2).

To avoid kinetic trapping, cooling was also performed slowly, in a step wise manner (5°C steps with 10 min incubations at each step). Indeed, recovery of enzyme activity by this slow stepwise approach was significantly higher than by rapid cooling. For example, after 30 min incubations of 10 μM TtC-G at T_m , the residual activity was 64% after rapid cooling relative to 86% after stepwise cooling. In this case, the 14% activity loss may be due to an irreversibly inactivated state *I*. The residual activity analysis performed by such a stepwise cooling revealed a simple one step thermal inactivation of TtC-G at 10 μM concentration (Fig. 5). No such cooling method-dependent differences were detected with AoC, suggesting that kinetic trapping did not play a role in AoC thermal inactivation (data not shown). Like AoC and TtC-NG, LC-MS analysis showed TtC-G's loss in residual activity during incubations at 67°C is not due to chemical degradation (data not shown).

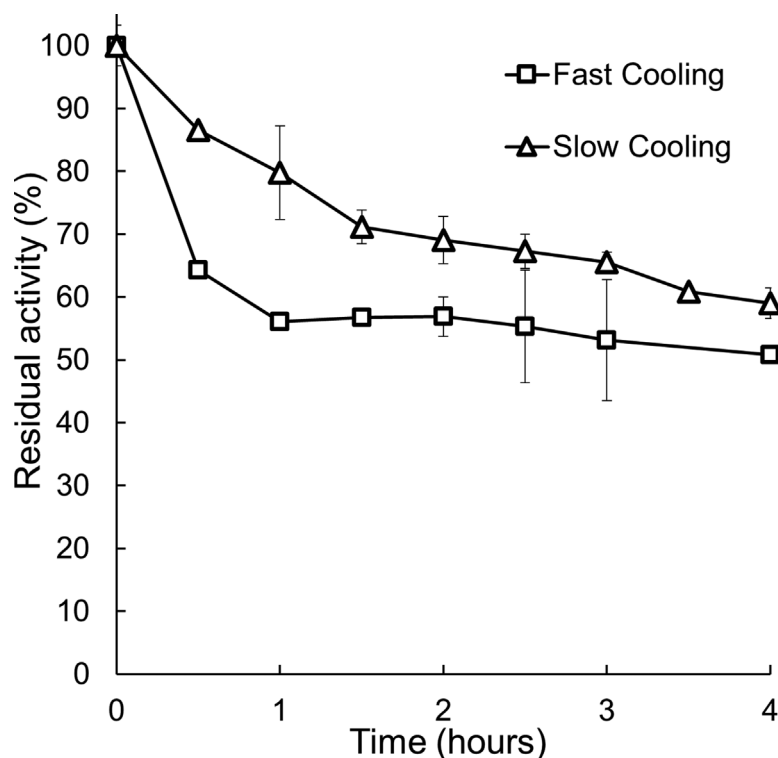
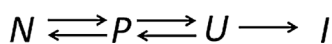


Figure 5. Residual activity analysis of TtC-G at 10 μ M with slow (5°C steps with 10 min incubations at each step) and fast (immediately quenched in ice) cooling from the apparent T_m at 67°C (continuous lines are used to guide the eyes).

The above analysis of TtC-G thermal inactivation is captured in Scheme 5 where thermal unfolding of the native protein (N) occurs through a partially unfolded intermediate state (P) to the completely unfolded state (U) which, depending on the temperature and the incubation time, results in formation of the irreversibly unfolded state (I). It is intriguing to consider that the stabilization of TtC by glycosylation, which effectively inhibited thermal aggregation, may be a generally applicable strategy for cutinase thermostabilization.



Scheme 5.

Unified Model for Cutinases

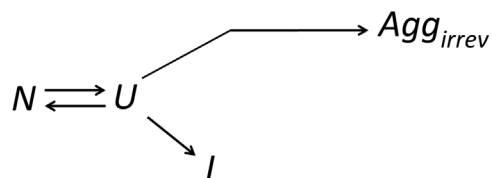
Based on the data reported in this study and publications on FsC (Baptista et al., 2003), aggregation seeded by thermal unfolding was found to play an important role in cutinase thermal inactivation. We propose that inactivation of the cutinase homologues AoC, TtC, and FsC can be represented by a unified model (Fig. 6). However, amongst these cutinases, variations are seen in the dominant inactivation pathways. Figure 6 summarizes thermal deactivation pathways of AoC, TtC, and FsC. Interestingly, the largest deviation from the unified model was not caused by variations in cutinase amino acid sequence, but, instead, by glycosylation of TtC.

Thermostabilization of AoC by Glycosylation Site Engineering

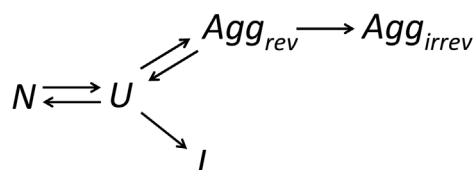
Inspired by the example of TtC-G, glycosylation site engineering of AoC was studied. Also, the stability of glycosylated AoC was compared to the stabilization that can be achieved by simply adding trehalose to AoC. Indeed, the addition of sugars and other additives have frequently been used to inhibit thermal aggregation (Sola-Penna and Meyer-Fernandes, 1998). Strategies for determining sites at which glycans are best introduced to stabilize the corresponding protein have targeted protein positions such as loop regions (Shental-Bechor and Levy, 2009) and hydrophobic patches (Sagt et al., 2000). Herein, the high sequence homology of AoC and TtC (56%) was exploited to guide the positioning of glycans for AoC. TtC has two glycosylation sites, N195 and N127, the corresponding locations on AoC are L185 and D117. Between these two locations, L185 was selected owing to the higher sequence similarity between AoC and TtC-G in the vicinity of L185 as compared to D117 (See Fig. S8A). Moreover, a single mutation (L185N) is sufficient to build a consensus sequence (Asn-Gly-Thr) for glycosylation. The desired mutation was introduced by site directed mutagenesis. The glycosylation site variant of AoC (AoC-G) was successfully expressed in *Pichia pastoris* and the presence of glycosylation was confirmed by SDS PAGE analysis coupled with glycopeptide staining (Fig. S9).

Preliminary characterization of AoC-G hydrolysis activity was performed using poly(ϵ -caprolactone), PCL, as the substrate.

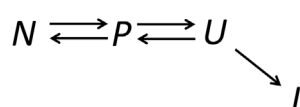
Fusarium solani Cutinase



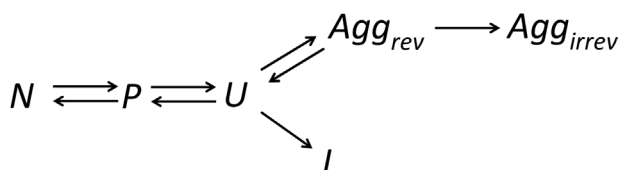
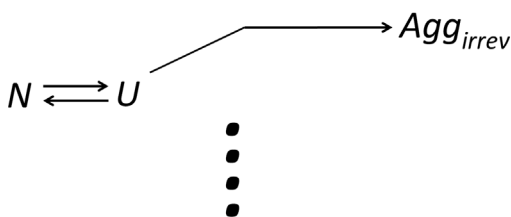
Aspergillus oryzae Cutinase



Thiellavia terrestris Cutinase (glycosylated)



Thiellavia terrestris Cutinase (non-glycosylated)



Cutinases

Figure 6. Proposed kinetic models of cutinase thermal inactivation.

Additional characterizations of AoC-G were performed by CD wavelength and temperature scans and a DLS thermal scan followed by residual activity analysis at the apparent T_m . Unfortunately, AoC-G was found to be less active than wt-AoC. The catalytic efficiency of AoC-G ($K \times k_{cat}$) is 75% that of wt-AoC (See Table SI 3). The CD secondary structure analysis revealed no significant differences between wt-AoC and AoC-G (Fig. S10). Thus the observed activity loss may be due to steric effects given the proximity of the introduced glycan to the active site (Shirke et al., 2016) (see Fig. S8A and B). Furthermore, the CD temperature scan of AoC-G revealed that its apparent T_m is similar to that of wt-AoC ($T_m = 61^\circ\text{C}$) (Fig. 7A). Moreover, the thermal unfolding profiles of wt-AoC and AoC-G from CD temperature scans are similar in contrast to large differences between those of TtC-G and TtC-NG (Figs. 2 and 7A). This

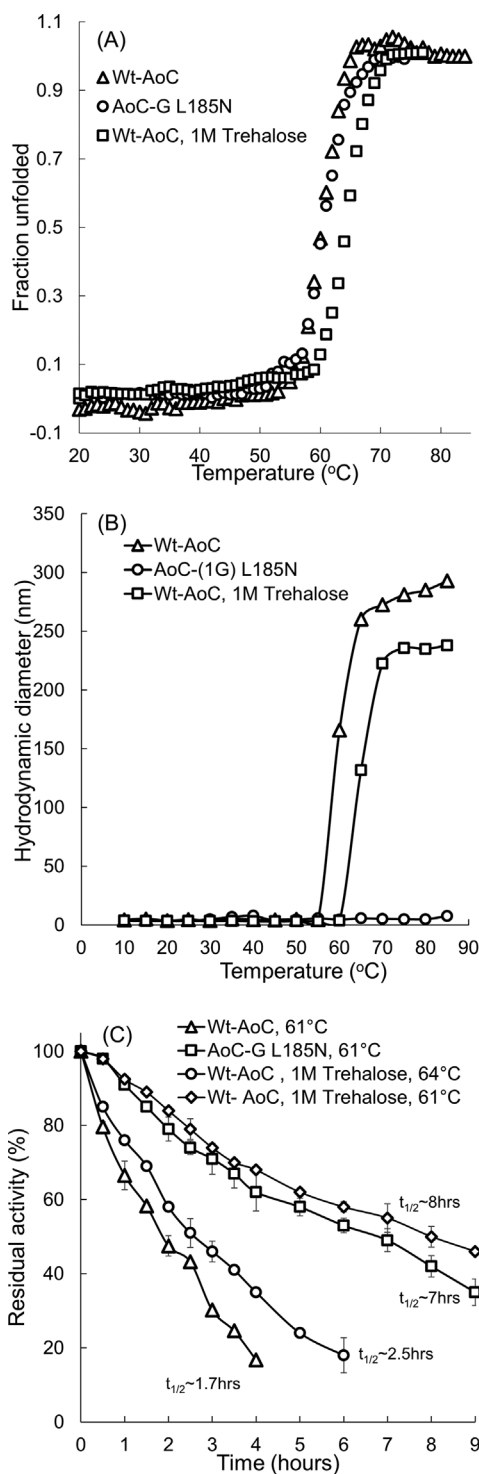


Figure 7. Comparative thermostability of $10 \mu\text{M}$ wt-AoC and AoC-G solutions in 20 mM phosphate buffer (pH 8) in the presence and absence of 1 M trehalose: (A) CD temperature scan; (B) DLS temperature scan; and (C) residual activity analysis at respective apparent T_m (continuous lines are used to guide the eyes).

dissimilarity between TtC-G and AoC-G may be due to the presence of two glycosylation sites in the former versus only one in later. Moreover, AoC and TtC display significant sequence variation (44%) which may also contribute to this dissimilarity.

Among the most evident effects of glycosylation, the DLS temperature scan of 10 μ M AoC-G revealed no transition when heated well above its T_m . In contrast, the onset of thermal aggregation of wt-AoC begins at the start of thermal unfolding based on the CD temperature scan (Fig. 7A and B). Hence, glycosylation of AoC at one site resulted in the inhibition of thermal aggregation. Indeed, this stabilization against aggregation resulted in improved AoC-G kinetic stability, where the $t_{1/2}$ for inactivation at 61°C is \sim 4 times larger than that of wt-AoC (Fig. 7C). While glycosylation of AoC was found to be a promising strategy to increase the resistance of AoC against thermal aggregation, the accompanying loss in enzyme activity is undesirable. However, we expect that the loss in activity by glycosylation can be avoided by rationally designing the glycosylation site (e.g., selecting locations far from the active site).

The thermostabilization of AoC by use of chemical additives was evaluated. Trehalose at 1 M is commonly used for protein stabilization (Sola-Penna and Meyer-Fernandes, 1998). It is an osmolyte with a complex mechanism of stabilization. Trehalose is known to stabilize FcC by shifting the equilibrium between *N* and *U* towards *N*, primarily due to excluded volume effects (Baptista et al., 2008). The presence of 1 M trehalose resulted in a 6°C increase in the T_m of FcC (Baptista et al., 2008). Figure 7A shows that addition of 1 M trehalose results in a 3°C increase (61 to 64°C) in wt-AoC T_m . This increase is also likely due to excluded volume effects. Furthermore, 1 M trehalose increased the $t_{1/2}$ for wt-AoC inactivation from 1.7 (without trehalose) to 8 h, a \sim 5 time increase (Fig. 7C). The improved kinetic stability at 61°C with 1 M trehalose is primarily due to retention of $>90\%$ of the proteins native state at 61°C as opposed to 50% retention of native state conformation in the absence of trehalose. Correspondingly, $t_{1/2}$ for wt-AoC at 64°C with trehalose and wt-AoC at 61°C without trehalose are similar (2.5 and 1.7 h, respectively).

Thermal aggregation analysis of wt-AoC in presence of trehalose shows a transition that occurs at (\sim 3–4°C) above that in the absence of trehalose (Fig. 7B). This shift in the aggregation temperature corresponds with the 3°C increase in the thermal unfolding temperature by adding 1 M trehalose. This is consistent with the large decrease in $t_{1/2}$ for wt-AoC with 1 M trehalose by conducting the thermostability analysis at 64°C as opposed to 61°C (Fig. 7C). In other words, at 64 and 61°C, retention of the wt-AoC native state with 1 M trehalose is about 50 and 90%, respectively. Greater AoC unfolding results in more rapid formation of irreversible aggregates that decreases $t_{1/2}$. Similar behavior was observed for wt-AoC (in the absence of trehalose) but not AoC-G where thermal aggregation is completely inhibited (Figs. 4B and 7B).

The results above demonstrate that the extent of AoC thermal aggregation inhibition is greater when a mannose rich glycan is covalently attached to AoC than when trehalose (1 M) is added to the AoC solution. Previous work by others confirms that covalent attachment of sugars to proteins can lead to stabilization that is equal to or exceeds that attained by use of sugar additives. The authors attributed this effect to the ability of the covalently attached sugar to more strongly influence the proteins microenvironment relative to the high concentrations of sugars in protein solution (Swanwick et al., 2005). Glycosylation by *P. pastoris* leads to covalent attachment of hydrophilic mannose rich oligomers that consist of 25–50 units

(Bretthauer and Castellino, 1999). The interactions of a covalently attached glycan with amino acid side chains of the protein was shown to result in thermodynamic stabilization with improvement in T_m (Barb et al., 2010; Culyba et al., 2011). However, the absence of an enhancement in AoC-G's T_m relative to the non-glycosylated form indicates that such interactions that might provide thermodynamic stabilization by glycosylation are small or non-existent. Thus, as discussed above for TtC-G, stabilization against aggregation is likely to be a result of inhibition of protein–protein interactions owing to steric constraints imposed by the glycans. In contrast, trehalose primarily stabilizes the proteins native state or results in excluded volume effects which do not substantially influence protein–protein interactions. Consequently, upon unfolding, protein–protein interactions lead to aggregation. Higher stabilizing effect of trehalose can be expected at higher concentrations (>1 M that is used in this study); which, based on the current analysis we believe will primarily be further improvement in T_m rather than total inhibition of the thermal aggregation.

Thus, for aggregation prone enzymes such as cutinases, glycosylation is particularly useful to combat thermal aggregation as compared to use of trehalose, however, different benefits could be gained from the later.

Conclusions

In this study, we describe a common thermal inactivation pathway for fungal cutinase homologues. In general, thermal aggregation is a dominating pathway for cutinase thermal inactivation that occurs in parallel with thermal unfolding at higher temperatures ($\geq T_m$). Thus, inhibition of the thermal unfolding is crucial to cutinase thermostabilization. Considering the small variation among inactivation profiles of these homologues (AoC, TtC, and FcC), it is likely that the common thermal inactivation pathway will also be applicable to other homologues with significant sequence identity ($>40\%$). Hence, this paper provides insights into strategies that can be followed for related enzymes to improve their thermostability.

Glycosylation of TtC contributes to the total inhibition of its thermal aggregation which resulted in 5–15 time (dependent on protein concentration) improvements in the kinetic stability of TtC at its apparent T_m . The lesson learned from the stability of TtC-G was successfully applied for the thermostabilization of AoC. Incorporation of just one glycosylation site designed based on the sequence alignment with TtC was sufficient to completely inhibit thermal aggregation of AoC resulting in \sim 4 time improvement in its kinetic stability at its apparent T_m . Further, the glycosylation of cutinases was more effective than use of the additive trehalose for thermostabilization. The ability to circumvent the use of additives is economically preferable.

References

- Arakawa T, Timasheff SN. 1982. Stabilization of protein structure by sugars. *Biochemistry* 21:6536–6544.
- Arakawa T, Timasheff SN. 1985. The stabilization of proteins by osmolytes. *Biophys J* 47:411–414.
- Badenes SM, Lemos F, Cabral JM. 2010. Transesterification of oil mixtures catalyzed by microencapsulated cutinase in reversed micelles. *Biotechnol Lett* 32:399–403.

- Baker PJ, Poultney C, Liu Z, Gross R, Montclare JK. 2012. Identification and comparison of cutinases for synthetic polyester degradation. *Appl Microbiol Biotechnol* 93:229–240.
- Baptista RP, Chen LY, Paixão A, Cabral JM, Melo EP. 2003. A novel pathway to enzyme deactivation: The cutinase model. *Biotechnol Bioeng* 82:851–857.
- Baptista RP, Pedersen S, Cabrita GJ, Otzen DE, Cabral JM, Melo EP. 2008. Thermodynamics and mechanism of cutinase stabilization by trehalose. *Biopolymers* 89:538–547.
- Barb AW, Borgert AJ, Liu M, Barany G, Live D. 2010. Intramolecular Glycan-Protein interactions in glycoproteins. In: Fukuda M, editor. *Methods in enzymology*. Cambridge: Academic Press. p 365–388.
- Barth M, Wei R, Oeser T, Then J, Schmidt J, Wohlgemuth F, Zimmermann W. 2015. Enzymatic hydrolysis of polyethylene terephthalate films in an ultrafiltration membrane reactor. *J Membr Sci* 494:182–187.
- Baynes BM, Trout BL. 2004. Rational design of solution additives for the prevention of protein aggregation. *Biophys J* 87:1631–1639.
- Benjwal S, Verma S, Röhm KH, Gurusy O. 2006. Monitoring protein aggregation during thermal unfolding in circular dichroism experiments. *Protein Sci* 15:635–639.
- Bennion BJ, Daggett V. 2003. The molecular basis for the chemical denaturation of proteins by urea. *Proc Natl Acad Sci USA* 100:5142–5147.
- Brethauer RK, Castellino FJ. 1999. Glycosylation of *Pichia pastoris*-derived proteins. *Biotechnol Appl Biochem* 30:193–200.
- Carrion-Vazquez M, Oberhauser AF, Fowler SB, Marszalek PE, Broedel SE, Clarke J, Fernandez JM. 1999. Mechanical and chemical unfolding of a single protein: A comparison. *Proc Natl Acad Sci USA* 96:3694–3699.
- Carvalho CM, Aires-Barros MR, Cabral JM. 2000. Kinetics of cutinase catalyzed transesterification in AOT reversed micelles: Modeling of a batch stirred tank reactor. *J. Biotechnol.* 81:1–13.
- Chen S, Su L, Chen J, Wu J. 2013. Cutinase: Characteristics, preparation, and application. *Biotechnol. Adv.* 31:1754–1767.
- Chi EY, Krishnan S, Randolph TW, Carpenter JF. 2003. Physical stability of proteins in aqueous solution: Mechanism and driving forces in nonnative protein aggregation. *Pharm Res* 20:1325–1336.
- Culyba EK, Price JL, Hanson SR, Dhar A, Wong C-H, Gruebele M, Powers ET, Kelly JW. 2011. Protein native-state stabilization by placing aromatic side chains in N-glycosylated reverse turns. *Science* 331:571–575.
- De Barros DP, Fonseca LP, Cabral JM, Weiss CK, Landfester K. 2009. Synthesis of alkyl esters by cutinase in miniemulsion and organic solvent media. *Biotechnol J* 4:674–683.
- De Barros DP, Azevedo AM, Cabral Fonseca JMLP. 2012. Optimization of flavor esters synthesis by *fusarium solani pisi* cutinase. *J Food Biochem* 36: 275–284.
- DeKoster GT, Robertson AD. 1997. Thermodynamics of unfolding for Kazal-type serine protease inhibitors: Entropic stabilization of ovomucoid first domain by glycosylation. *Biochemistry* 36:2323–2331.
- Devi NA, Rao AGA. 1998. Effect of additives on kinetic thermal stability of polygalacturonase II from *Aspergillus carbonarius*: Mechanism of stabilization by sucrose. *J. Agric. Food Chem.* 46:3540–3545.
- Eberl A, Heumann S, Brückner T, Araujo R, Cavaco-Paulo A, Kaufmann F, Kroutil W, Guebitz GM. 2009. Enzymatic surface hydrolysis of poly(ethylene terephthalate) and bis(benzoyloxyethyl) terephthalate by lipase and cutinase in the presence of surface active molecules. *J. Biotechnol.* 143:207–212.
- Ellis CR, Maiti B, Noid WG. 2012. Specific and nonspecific effects of glycosylation. *J. Am. Chem. Soc.* 134:8184–8193.
- Fagain CO. 1995. Understanding and increasing protein stability. *Biochim. Biophys. Acta – Protein Struct. Mol. Enzymol.* 1252:1–14.
- Fields PA. 2001. Review: Protein function at thermal extremes: Balancing stability and flexibility. *Comp. Biochem. Physiol. Part A Mol. Integr. Physiol.* 129:417–431.
- Fonseca-Maldonado R, Vieira DS, Alponi JS, Bonheil E, Thibault P, Ward RJ. 2013. Engineering the pattern of protein glycosylation modulates the thermostability of a GH11 xylanase. *J. Biol. Chem.* 288:25522–25534.
- Gübitz GM, Paulo AC. 2003. New substrates for reliable enzymes: Enzymatic modification of polymers. *Curr Opin Biotechnol* 14:577–582.
- Gouda MD, Singh SA, Rao AA, Thakur MS, Karanth NG. 2003. Thermal inactivation of glucose oxidase: Mechanism and stabilization using additives. *J Biol Chem* 278:24324–24333.
- Højberg-Nielsen R, Fuglsang CC, Arleth L, Westh P. 2006. Interrelationships of glycosylation and aggregation kinetics for peniophora lycii phytase. *Biochemistry* 45:5057–5066.
- Højberg-Nielsen R, Westh P, Skov LK, Arleth L. 2009. Interrelationship of steric stabilization and self-crowding of a glycosylated protein. *Biophys J* 97:1445–1453.
- Hayakawa I, Linko YY, Linko P. 1996. Mechanism of high pressure denaturation of proteins. *LWT – Food Sci Technol* 29:756–762.
- Imperiali B, O'Connor SE. 1999. Effect of N-linked glycosylation on glycopeptide and glycoprotein structure. *Curr Opin Chem Biol* 3:643–649.
- Jain NK, Roy I. 2009. Effect of trehalose on protein structure. *Protein Sci* 18:24–36.
- Kaushik JK, Bhat R. 1998. Thermal stability of proteins in aqueous polyol solutions: Role of the surface tension of water in the stabilizing effect of polyols. *J Phys Chem B* 5647:7058–7066.
- Kazenwadel C, Eiben S, Maurer S, Beuttler H, Wetzl D, Hauer B, Koschorreck K. 2012. Thiol-functionalization of acrylic ester monomers catalyzed by immobilized *Humicola insolens* cutinase. *Enzyme Microb Technol* 51:9–15.
- Koutsopoulos S, van der Oost J, Norde W. 2007. Kinetically controlled refolding of a heat-denatured hyperthermostable protein. *FEBS J* 274:5915–5923.
- Lee SH, Song WS. 2010. Surface modification of polyester fabrics by enzyme treatment. *Fibers Polym* 11:54–59.
- Leskovic V. 2003. Effects of Temperature on Enzyme Reactions In: *Compr. Enzym. Kinet.* Boston: Kluwer Academic Publishers. p 317–327.
- Liu Z, Gosser Y, Baker PJ, Ravee Y, Lu Z, Alemu G, Li H, Butterfoss GL, Kong XP, Gross R, Montclare JK. 2009. Structural and functional studies of *Aspergillus oryzae* cutinase: Enhanced thermostability and hydrolytic activity of synthetic ester and polyester degradation. *J Am Chem Soc* 131:15711–15716.
- Lumry R, Eyring R. 1954. Conformation changes of proteins. *J Phys Chem* 58:110–120.
- Matthews BW. 1993. Structural and genetic analysis of protein stability. *Annu Rev Biochem* 62:139–160.
- Mozhaev VV. 1993. Mechanism-based strategies for protein thermostabilization. *Trends Biotechnol* 11:88–95.
- Otzen DE. 2002. Protein unfolding in detergents: Effect of micelle structure, ionic strength, pH, and temperature. *Biophys J* 83:2219–2230.
- Pace CN. 1992. Contribution of the hydrophobic effect to globular protein stability. *J Mol Biol* 226:29–35.
- Pio TF, Macedo GA. 2009. Cutinases: Properties and industrial applications. *Adv Appl Microbiol* 66:77–95.
- Polizzi KM, Bommarius AS, Broering JM, Chaparro-Riggers JF. 2007. Stability of biocatalysts. *Curr Opin Chem Biol* 11:220–225.
- Querol E, Perez-Pons JA, Mozo-Villarias A. 1996. Analysis of protein conformational characteristics related to thermostability. *Protein Eng* 9:265–271.
- Robertson AD, Murphy KP. 1997. Protein structure and the energetics of protein stability. *Chem Rev* 97:1251–1268.
- Rodriguez-Larrea D, Ibarra-Molero B, de Maria L, Borchert TV, Sanchez-Ruiz JM. 2007. Beyond Lumry-Eyring: An unexpected pattern of operational reversibility/irreversibility in protein denaturation. *Proteins: Struct, Funct, Bioinf* 70:19–24.
- Sagt CM, Kleizen B, Verwaal R, De Jong MD, Müller WH, Smits A, Visser C, Boonstra J, Verkleij AJ, Verrips CT. 2000. Introduction of an N-glycosylation site increases secretion of heterologous proteins in yeasts. *Appl Environ Microbiol* 66:4940–4944.
- Sanchez-Ruiz JM. 1992. Theoretical analysis of Lumry-Eyring models in differential scanning calorimetry. *Biophys J* 61:921–935.
- Sanchez-Ruiz JM. 2010. Protein kinetic stability. *Biophys Chem* 148:1–15.
- Shental-Bechor D, Levy Y. 2008. Effect of glycosylation on protein folding: A close look at thermodynamic stabilization. *Proc Natl Acad Sci USA* 105:8256–8261.
- Shental-Bechor D, Levy Y. 2009. Folding of glycoproteins: Toward understanding the biophysics of the glycosylation code. *Curr Opin Struct Biol* 19:524–533.
- Shirke AN, Basore D, Holton S, Su A, Baugh E, Butterfoss GL, Makhatadze G, Bystroff C, Gross RA. 2016. Influence of surface charge, binding site residues and glycosylation on *Thielavia terrestris* cutinase biochemical characteristics. *Appl Microbiol Biotechnol* 100(10):4436–4446.
- Shortle DA. 1996. The denatured state (the other half of the folding equation) and its role in protein stability. *FASEB J* 10:27–34.
- Sizer IW. 2006. Effects of temperature on enzyme kinetics. *Adv Enzymol Relat Areas Mol Biol* 3:35–62.

- Solá RJ, Griebenow K. 2010. Effects of glycosylation on the stability of protein pharmaceuticals. *J Pharm Sci* 98:1223–1245.
- Solá RJ, Al-Azzam W, Griebenow K. 2006. Engineering of protein thermodynamic, kinetic, and colloidal stability: Chemical glycosylation with monofunctionally activated glycans. *Biotechnol Bioeng* 94:1072–1079.
- Sola-Penna M, Meyer-Fernandes JR. 1998. Stabilization against thermal inactivation promoted by sugars on enzyme structure and function: Why is trehalose more effective than other sugars? *Arch Biochem Biophys* 360:10–14.
- Somero GN. 1995. Proteins and temperature. *Annu Rev Physiol* 57:43–68.
- Stelea SD, Keiderling TA. 2002. Pretransitional structural changes in the thermal denaturation of ribonuclease S and S protein. *Biophys J* 83:2259–2269.
- Swanwick RS, Daines AM, Tey LH, Flitsch SL, Allemann RK. 2005. Increased thermal stability of site-selectively glycosylated dihydrofolate reductase. *ChemBioChem* 6:1338–1340.
- Tams JW, Welinder KG. 1998. Glycosylation and thermodynamic versus kinetic stability of horseradish peroxidase. *FEBS Lett* 421:234–236.
- Tams JW, Welinder KG. 2001. Kinetic stability of designed glycosylation mutants of coprinus cinereus peroxidase. *Biochem Biophys Res Commun* 286:701–706.
- Timasheff SN. 1993. The control of protein stability and association by weak interactions with water: How do solvents affect these processes? *Annu Rev Biophys Biomol Struct* 22:67–97.
- Vertommen MA, Nierstrasz VA, Van der Veer M, Warmoeskerken MM. 2005. Enzymatic surface modification of poly(ethylene terephthalate). *J Biotechnol* 120:376–386.
- Vieille C, Zeikus GJ. 2001. Hyperthermophilic enzymes: Sources, uses, and molecular mechanisms for thermostability. *Microbiol Mol Biol Rev* 65:1–43.
- Wang C, Eufemi M, Turano C, Giartosio A. 1996. Influence of the carbohydrate moiety on the stability of glycoproteins. *Biochemistry* 35:7299–7307.
- Wei R, Oeser T, Barth M, Weigl N, Lübs A, Schulz-Siegmund M, Hacker MC, Zimmermann W. 2013. Turbidimetric analysis of the enzymatic hydrolysis of polyethylene terephthalate nanoparticles. *J Mol Catal B Enzym* 103:72–78.
- Yan YB, Wang Q, He HW, Hu XY, Zhang RQ, Zhou HM. 2003. Two-dimensional infrared correlation spectroscopy study of sequential events in the heat-induced unfolding and aggregation process of myoglobin. *Biophys J* 85:1959–1967.
- Yang AS, Honig B. 1993. On the pH dependence of protein stability. *J Mol Biol* 231:459–474.
- Yang S, Xu H, Yan Q, Liu Y, Zhou P, Jiang Z. 2013. A low molecular mass cutinase of *Thielavia terrestris* efficiently hydrolyzes poly(esters). *J Ind Microbiol Biotechnol* 40:217–226.
- Yang H, Liu L, Li J, Chen J, Du G. 2015. Rational design to improve protein thermostability: Recent advances and prospects. *ChemBioEng Rev* 2:87–94.
- Zhang Y, Chen S, Wu J, Chen J. 2012. Enzymatic surface modification of cellulose acetate fibre by cutinase-CBM (carbohydrate-binding module) fusion proteins. *Biocatal Biotransform* 30:184–189.
- Zhong X, Somers W. 2012. Recent advances in glycosylation modifications in the context of therapeutic glycoproteins. In: Leung HE editor. *Integr. proteomics*. Rijeka: InTech. p 183–196.
- Zoldák G, Zubrik A, Musatov A, Stupák M, Sedlák E. 2004. Irreversible thermal denaturation of glucose oxidase from *Aspergillus niger* is the transition to the denatured state with residual structure. *J Biol Chem* 279:47601–47609.

Supporting Information

Additional supporting information may be found in the online version of this article at the publisher's web-site.